Available online at www.sciencedirect.com
ScienceDirect
Journal of Sound and Vibration 310 (2008) 855–864
JOURNAL OF SOUND AND VIBRATION
www.elsevier.com/locate/jsvi

Study on the chaos anti-control technology in nonlinear vibration isolation system

Shu-Yong Liu*, Xiang Yu, Shi-Jian Zhu

Institute of Noise & Vibration, Naval University of Engineering, Wuhan 430033, China

Received 18 January 2007; received in revised form 4 August 2007; accepted 7 August 2007
Available online 20 September 2007

Abstract

The nonlinear vibration isolation system (NVIS) works in a chaotic state when its parameters are in chaotic range. Under single-frequency harmonic excitation, the system exhibits chaotic behavior with broad band frequency. This idea can be used to control the line spectra water-born noise of the underwater vehicle, and to improve its capability of concealment. In order to ensure that the system works in the chaotic state effectively, a new chaos anti-control method is presented in this paper. Firstly, the NVIS model with feedback is provided, and the periodic-doubling bifurcation characteristic is analyzed. Simulation results show that the system has multiple dynamical behaviors with different parameters. Finally, an experiment on the basis of self-design rig is carried out, and the acceleration signal is measured. Combined with the chaos identification technology, it proves that the system works in a chaotic state at some special parameter range.
© 2007 Elsevier Ltd. All rights reserved.

1. Introduction

With the development of the chaos theory, how to control chaos becomes an important problem in engineering. OGY chaos controlling method was presented in Ref. [1]. The main idea is to determine the unstable periodic orbit in the reconstructed attractor firstly, and choose one of them as controlling target. Then, the chaotic orbit is stabilized on the special periodic one by taking small perturbation. This method, however, is mainly applied to control harmful chaos in practice. In fact, chaos is found to be a useful technology in many fields. At present, chaos in the well-known engineering fields, including chaos synchronization in security communication [2], chaotic roller, and chaotic vibration griddle and so on, has been researched extensively. The important procedure in these applications is how to realize chaotification [3–5], and then the special chaotic state is obtained. Tang et al. [6] analyzed the role of the $x|x|$ term in chaos anti-control for the autonomous system, and results show that most of the piecewise system with cubic nonlinear factor can exhibit chaotic behavior. The delay feedback control method [7] was applied in the continuous-time minimum phase system chaotic by Wang et al., [8] and they researched how to chaotify a stable LTI system by tiny feedback control. Yang et al. [9] studied how to apply the impulsive input method to

*Corresponding author.
E-mail address: lsydh@sina.com (S.-Y. Liu).

0022-460X/$ - see front matter © 2007 Elsevier Ltd. All rights reserved.
doi:10.1016/j.jsv.2007.08.006

control chaos in a continuous-time system. Lou et al. [10] have studied the application of the chaos in vibration isolation system design, and they discussed how line spectra water-born noise of the warship can be reduced. In order to ensure that the system works in a chaotic state, it is important to determine its parameters range in the design. The traditional method is to analyze the system with nonlinear theory and then predict the chaotic parameters range. However, the difference between the predicted range and the practical one is remarkable because of the complexity of the nonlinear system. And thus the isolators with adjustable parameters must be applied in the system. The nonlinear vibration isolation system (NVIS) with feedback parts is presented in this paper. The system can be adjusted to work in the chaotic state by changing the feedback gain.

2. Modeling of the NVIS

In general, the periodic linear spectrum contained in the water-born noise is mainly produced by periodic excitation of machines, such as diesel engine, gas turbine and speed-down gears [11]. Fig. 1 illustrates the model of a vibration isolation system. In order to simplify the analysis, the weak interferences are neglected. The physical system is modeled as a single degree of freedom, damped oscillator subject to external excitation $F\cos\Omega T$, and the following equation is obtained:

$$M\ddot{X} + C\dot{X} + N(X) = F\cos\Omega T, \tag{1}$$

where $\ddot{X} = \mathrm{d}^2X/\mathrm{d}T^2$, $\dot{X} = \mathrm{d}X/\mathrm{d}T$ and $M\ddot{X}$, $C\dot{X}$, $N(X)$ are the inertial force, damping force and elastic restoring force, respectively. When these forces are linear, Eq. (1) represents a linear vibration isolation system, and thus the response of the system is harmonic according to superposition principle, that is, the response has the same periodic spectrum component as the external excitation. However, if $N(X)$ equals to $KX + UX^3$, Eq. (1) becomes

$$M\ddot{X} + C\dot{X} + KX + UX^3 = F\cos\Omega T. \tag{2}$$

This equation represents an NVIS with linear damping force and nonlinear restoring force. When $U>0$, it is called hard stiffness, otherwise it is soft stiffness. Here, only the hard stiffness system is discussed.

By defining $\Omega_0 = \sqrt{M/K}$, $T = \Omega_0 t$, and $X = x\sqrt{K/U}$, Eq. (2) can be written as

$$\ddot{x} + x + x^3 = -\delta\dot{x} + \gamma\cos\omega t, \tag{3}$$

where $\ddot{x} = \mathrm{d}^2x/\mathrm{d}t^2$, $\dot{x} = \mathrm{d}x/\mathrm{d}t$, $\delta = C/\sqrt{MK}$, $\omega = \Omega\Omega_0$ and $\gamma = F/(K\sqrt{K/U})$.

It is obvious that Eq. (3) is Duffing's equation [12], and the corresponding state equation is

$$\begin{cases} \dot{x} = y, \\ \dot{y} = -x - x^3 - \delta\cdot y + \gamma\cos\omega t. \end{cases} \tag{4}$$

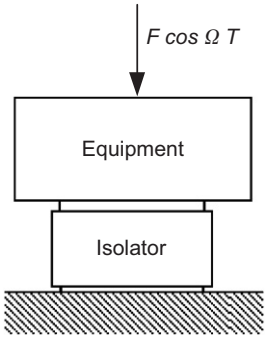

Fig. 1. Model of vibration isolation system.

3. Chaos anti-control method

For n-dimensional nonlinear system $\dot{\mathbf{x}} = \mathbf{f}(\mathbf{x}, t)$, where $\mathbf{f}$ is nonlinear smooth vector function, and $\mathbf{x}$ is the system state $\mathrm{x} = [x_1, x_2, \ldots, x_n]^{\mathrm{T}}$, the output of the system $y = \mathbf{cx}$, and $\mathbf{c}$ is $1 \times n$ constant matrix. The control law of the nonlinear feedback controller for the system is

$$Q = Gx, \tag{5}$$

where G is the feedback gain coefficient, and when the controller is applied to the nonlinear dynamic system, the controlled equation is obtained:

$$\dot{\mathbf{x}} = \mathbf{f}(\mathbf{x}, t) - Q. \tag{6}$$

When the gain coefficient is in a special range, the system can work in an expected state, and Eq. (4) can be rewritten as

$$\begin{cases} \dot{x} = y, \\ \dot{y} = -x - x^3 - \delta \cdot y + \gamma \cos \omega t - Gx. \end{cases} \tag{7}$$

Eq. (7) can also be written as

$$\begin{cases} \dot{x} = y, \\ \dot{y} = -(1 + G)x - x^3 - \delta \cdot y + \gamma \cos \omega t. \end{cases} \tag{7'}$$

4. Period-doubling bifurcation analysis of the NVIS with feedback control

The dynamical characteristic of system in Eq. (7) is analyzed first in this paper. It is clear that Eq. (7) looks like the hardening Duffing equation which has only one stable equilibrium point. Although the report of the nonlinear oscillator with one equilibrium point is presented in many references [13,14], the emphasis is always put on the chaos of the nonlinear system with two or three equilibrium points. E.H. Dowell and C. Pezeshki have studied the Holmes-type Duffing system with three equilibrium point and explained the mechanism of the chaos. Because the autonomous system corresponding to the hardening stiffness Duffing system has no homo- and hetero-clinic trajectory, there exists no chaos in the sense of the Smale horseshoe. The chaotic parameter range analysis is carried out in this paper, from the point of view of the period-doubling bifurcation.

For the hardening Duffing system, Eq. (7′) is rewritten as

$$\ddot{x} + \delta\dot{x} + (1 + G)x + x^3 = \gamma \cos(\omega t + \varphi), \tag{8}$$

where an initial phase angle φ is introduced, and the phase difference of the response can be transferred to the system equation to simplify the derivation. Suppose the zero-order approximate solution to Eq. (8) is

$$x(t) = a_0 \cos \omega t. \tag{9}$$

Substituting Eq. (9) into Eq. (8), we get

$$\begin{aligned} &\cos \omega t : \tfrac{3}{4}a_0^3 + a_0[(1 + G) - \omega^2] = g, \\ &\sin \omega t : \delta a_0 \omega = h, \end{aligned}$$

where $g = \gamma \cos \varphi$, $h = \gamma \sin \varphi$. In the derivation, the formula $\cos^3 \omega t = \frac{3}{4} \cos \omega t + \frac{1}{4} \cos 3\omega t$ is considered and the term containing high order harmonic $\cos 3\omega t$ is neglected. Because the amplitude a_0 in practical vibration is small, the high order term a_0^3 can be neglected, and then the parameters of the zero-order approximate solution are obtained: $a_0 = (\gamma \sin \varphi)/\delta\omega$ and $\varphi = \mathrm{arctg}(\delta\omega/(1 - \omega^2))$.

The perturbation method is applied to analyze the stability of period solution Eq. (9) first. If a small disturbance is added to Eqs. (9) and the following equation is obtained:

$$x(t) = \phi(t) + \eta(t), \tag{10}$$

where $\phi(t) = a_0 \cos \omega t$. Substitute Eq. (10) into Eq. (8), neglect the high-order term to obtain the following equation:

$$\ddot{\eta} + \delta\dot{\eta} + \eta\left[\frac{3a_0^2+2}{2}(1+G) + \frac{3a_0^2}{2}\cos 2\omega t\right] = 0. \tag{11}$$

As long as the solution to Eq. (11) is bounded, the period solution $\phi(t)$ is stable, vice versa. It is obvious that Eq. (11) is the differential equation with periodic coefficients. For this kind of second-order system, the Floquet theory is to be applied to study the stability of the solution. Firstly, Eq. (11) is transformed to Hill-type equation:

$$\ddot{x} + p(t)x = 0, \tag{12}$$

where $p(t) = \frac{1}{4}[(6a_0^2+4)(1+G) - \delta^2 + 6a_0^2 \cos 2\omega t]$. Substitute $T = \omega t$ into Eq. (12) and we get $(\mathrm{d}^2x/\mathrm{d}T^2) + (1/\omega^2)p(T)x(T) = 0$. Eq. (12) can be written as a Mathieu type equation:

$$\ddot{x} + (\delta' + 2\varepsilon \cos 2t)x = 0, \tag{13}$$

where

$$\delta' = \frac{(6a_0^2+4)(1+G) - \delta^2}{4\omega^2}, \quad \varepsilon = \frac{3a_0^2}{4\omega^2}. \tag{13'}$$

In order to determine the stable region of the period-doubling solution for Mathieu equation, the solution to Eq. (13) and parameter δ' are expanded in a power series of ε, and thus the following equations are obtained:

$$x(t,\varepsilon) = x_0(t) + \varepsilon x_1(t) + \varepsilon^2 x_2(t) + \ldots, \tag{14}$$

$$\delta' = \delta_0 + \varepsilon\delta_1 + \varepsilon^2\delta_2 + \ldots. \tag{15}$$

Substituting the two equations above into Eq. (13), and equating the coefficients of same powers, the following equations can be obtained:

$$\ddot{x}_0 + \delta_0 x_0 = 0, \tag{16a}$$

$$\ddot{x}_1 + \delta_0 x_1 = -\delta_1 x_0 - 2x_0 \cos 2t, \tag{16b}$$

$$\ddot{x}_2 + \delta_0 x_2 = -\delta_2 x_0 - 2x_1 \cos 2t - \delta_1 x_1. \tag{16c}$$

$$\vdots$$

Let $\delta_0 = n^2$ ($n = 0, 1, 2, \ldots$), and Eq. (16a) has periodic solution:

$$x_0 = a \cos nt + b \sin nt. \tag{17}$$

In order to discuss the period-doubling bifurcation, suppose $\delta_0 = 1$. Substitute Eq. (17) into Eq. (16b), and eliminate secular term. As a result, the following equations are obtained $x_1 = (1/8)a \cos 3t$ or $x_1 = (1/8)b \sin 3t$. Substituting them into Eq. (16c), we obtain

$$\begin{aligned} \ddot{x}_2 + \delta_0 x_2 &= -a\left(\delta_2 + \tfrac{1}{8}\right)\cos t + \tfrac{1}{8}a \cos 3t - \tfrac{1}{8}a \cos 5t, \\ \ddot{x}_2 + \delta_0 x_2 &= -b\left(\delta_2 + \tfrac{1}{8}\right)\sin t - \tfrac{1}{8}\sin 3t - \tfrac{1}{8}b \sin 5t. \end{aligned} \tag{18}$$

Because x_2 is a period solution, we can get $\delta_2 = -1/8$ from the equations above. And thus two boundaries are obtained:

$$\delta' = 1 - \varepsilon - \tfrac{1}{8}\varepsilon^2 + O(\varepsilon^3), \tag{19a}$$

$$\delta' = 1 + \varepsilon - \tfrac{1}{8}\varepsilon^2 + O(\varepsilon^3). \tag{19b}$$

They correspond to the following solutions:

$$x_1 = a\left(\cos t + \tfrac{1}{8}\varepsilon \cos 3t\right) + O(\varepsilon^2), \tag{20}$$

$$x_2 = b\left(\sin t + \tfrac{1}{8}\varepsilon \sin 3t\right) + O(\varepsilon^2). \tag{21}$$

Neglect square of small variable ε, substitute Eq. (13′) into Eqs. (19a) and (19b), and the range of the first period-doubling bifurcation is obtained

$$\sqrt{\omega_1^0} < \omega < \sqrt{\omega_2^0} \tag{22}$$

where

$$\omega_1^0 = \frac{\delta^2(4(1+G)-\delta^2) + \sqrt{\delta^4(4(1+G)-\delta^2) + 48\delta^2\gamma^2\sin^2\varphi}}{8\delta^2},$$

$$\omega_2^0 = \frac{\delta^2(4(1+G)-\delta^2) + \sqrt{\delta^4(4(1+G)-\delta^2) + 144\delta^2\gamma^2\sin^2\varphi}}{8\delta^2}.$$

Then, suppose the first-order approximate solution of Eq. (8) is

$$x(t) = a_1 \cos \omega t + b_1 \cos\left(\frac{\omega}{2}t + \theta\right). \tag{23}$$

The range of second period-doubling bifurcation can be evaluated. The system can enter chaotic range through many times of period-doubling bifurcation.

5. Simulations

In Eq. (7), set parameters as follows: $G = 0.1$, $\delta = 0.01$ and $\gamma = 28.28$. Then bifurcation diagram of the system, as shown in Fig. 2a, can be obtained by changing excitation frequency ω. When frequency $\omega < 0.12$, the system exhibits period-1 behavior. As the parameter ω is increased, the bifurcation solution appears, and the system exhibits multi-period behavior. In the range $0.5 < \omega < 0.97$, the response of the system is chaos at some values. When $\omega = 0.92$, the phase plane of the system is shown in Fig. 2b. It is a strange attractor [15,16], which is different from limit cycle or torus, and the Lyapunov exponent is 0.214. As ω approaches 1, system exhibits period-1 behavior once more. According to Eq. (7), the variation of gain parameter G can also change the system response. When the parameter $\omega = 0.9$ and is constant, and the parameter G is varied, the system

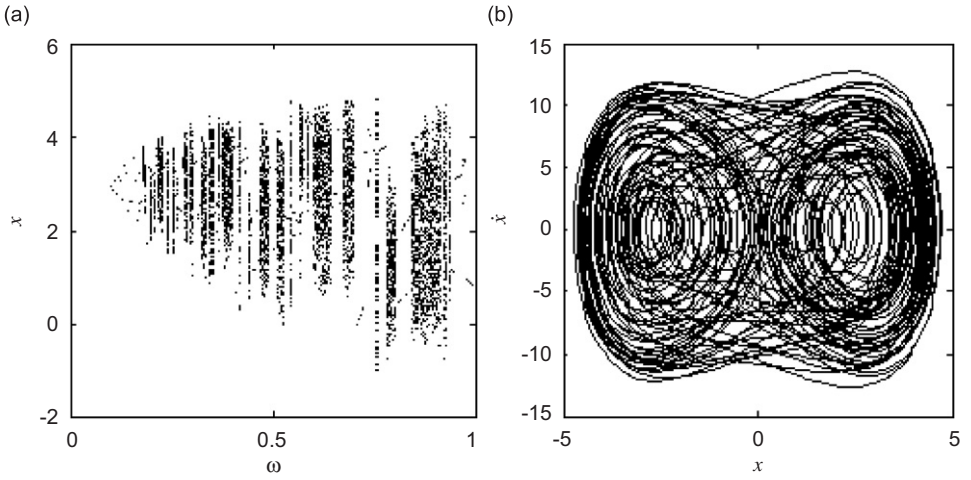

Fig. 2. Dynamic response of the system under different excitation frequency: (a) bifurcation diagram and (b) phase plane diagram.

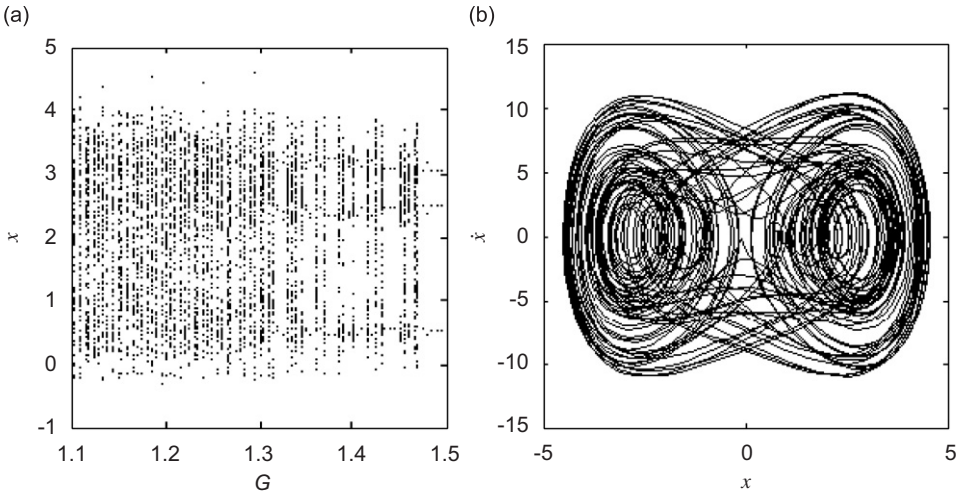

Fig. 3. Dynamic response of the system at different gain parameter: (a) bifurcation diagram and (b) phase plane diagram.

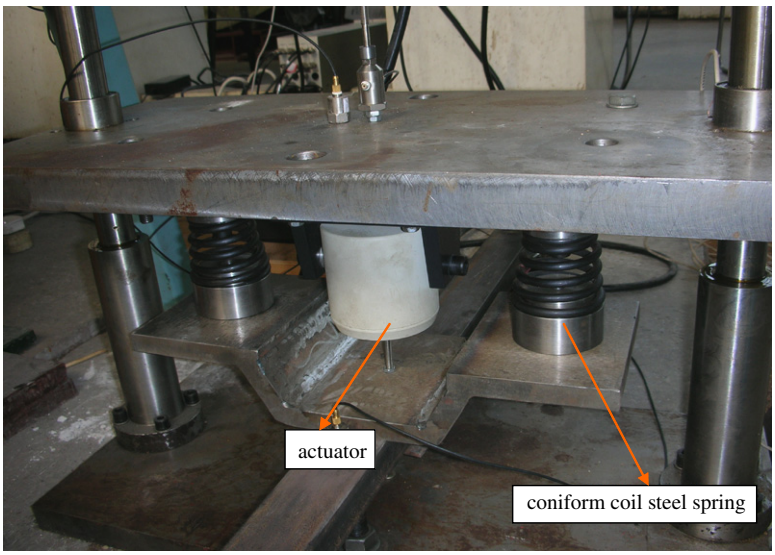

Fig. 4. Experimental rig of NVIS.

can work in a chaotic state in the range $G<1.3$, as shown in the bifurcation diagram (Fig. 3a. For example, when the gain $G = 1.22$, the system exhibits chaotic response, and the Lyapnov exponent is 0.153. As shown in Fig. 3b, the attractor is strange. In practical engineering, the system works in a special frequency, and hence the variation of G can reach the target of chaos anti-control according to the analysis above.

6. Experiment

The experiment is carried out on the self-design coniform coil steel spring NVIS, as shown in Figs. 4 and 5.

The test equipments include signal generator, power amplifier, actuator, acceleration sensor, signal measuring system (Pimento), computer (Fig. 6) etc. The acceleration sensor is used to measure the vibration signal of the system, and then it is transferred to the DSP. The output is applied to drive the actuator, and the gain coefficient can be adjusted. In practical engineering, the identification of chaotic vibration is very important. In general, the response of vibration isolation system such as velocity, acceleration can be measured by instruments. However, it is difficult to judge whether the state of system is chaotic or not by time

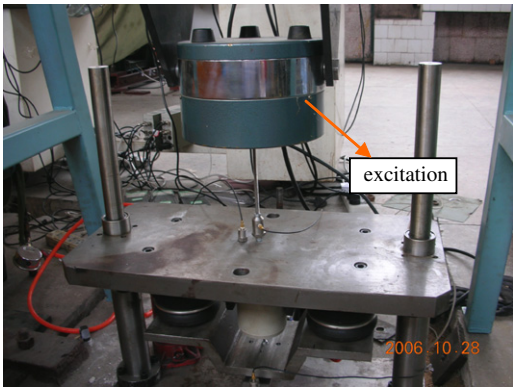

Fig. 5. Excitation source.

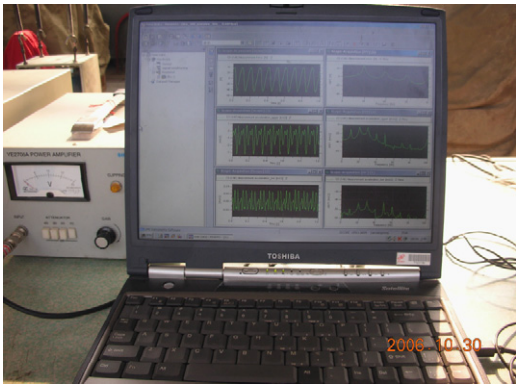

Fig. 6. Signal measuring system.

history. The power spectrum analysis is an efficient method to distinguish the periodic, multi-periodic and non-periodic signal. Clearly, the periodic and multi-periodic signal is regular and there are many peaks in the spectrum. The non-periodic signal is irregular and shows broadband spectrum. Chaotic signal is non-periodic, and can be distinguished from the regular one by power spectrum analysis. Compared with other indices such as fractal dimension, Lyapunov exponent [17], the power analysis, however, cannot be used to obtain the detailed information of the system. Hence, it is necessary to analyze the time series with comprehensive method.

Because the measured signal contains the information of all variables participating in the movement, the time series should be embedded in three or higher dimension phase space to characterize the dynamics of the original phase space. Then, the useful information can be revealed by phase space reconstruction. The trajectories in the space reflect the evolution of the system behavior. For regular signals, the attractor is a cycle in phase space. When signal is a chaotic time series, however, the attractor is strange, which has an irregular, complex and self-similar structure, i.e. it has fractal characteristic. The measured time series can be expressed by

$$x(t_0), x(t_1), x(t_2), \ldots, x(t_i) \in R, \tag{24}$$

where $t_i = t_0 + i\Delta t$. In order to obtain the geometrical structure of the dynamical system in the phase space, Packard et al. present a reconstruction technique, i.e. embedding the one-dimension time series in d-dimension space, and thus

$$Y(t) = [x(t), x(t+\tau), x(t+2\tau), \ldots, x(t+(d-1)\tau)], \tag{25}$$

where τ and d are time lag and embedding dimension respectively, $Y(t)$ is the dynamic state of the system at t. So a map between phase space R^M and R^d is constructed:

$$\varphi^{(d)} : R^M \to R^d. \tag{26}$$

Takens and Mañé [18] argue that if $d > 2D+1$ is satisfied, where d is an integer and D is fraction, the attractor in the reconstructed space will be smoothly related to the one in the unknown original physical coordinate. In the process of phase space reconstructing, it is critical to choose suitable parameters τ and d. If time lag τ is too small, the coordinates $x(t+j\tau)$ and $x(t+(j+1)\tau)$ will be so close to each other that they cannot be distinguished. Similarly, if τ is too large, $x(t+j\tau)$ and $x(t+(j+1)\tau)$ are completely independent in terms of statistics. As far as mutual information is concerned, if τ is too small, it will lead to information redundancy. If τ is too large, the mutual information $I(\tau)$ approaches to zero, that is, $x(t)$ and $x(t+\tau)$ are independent.

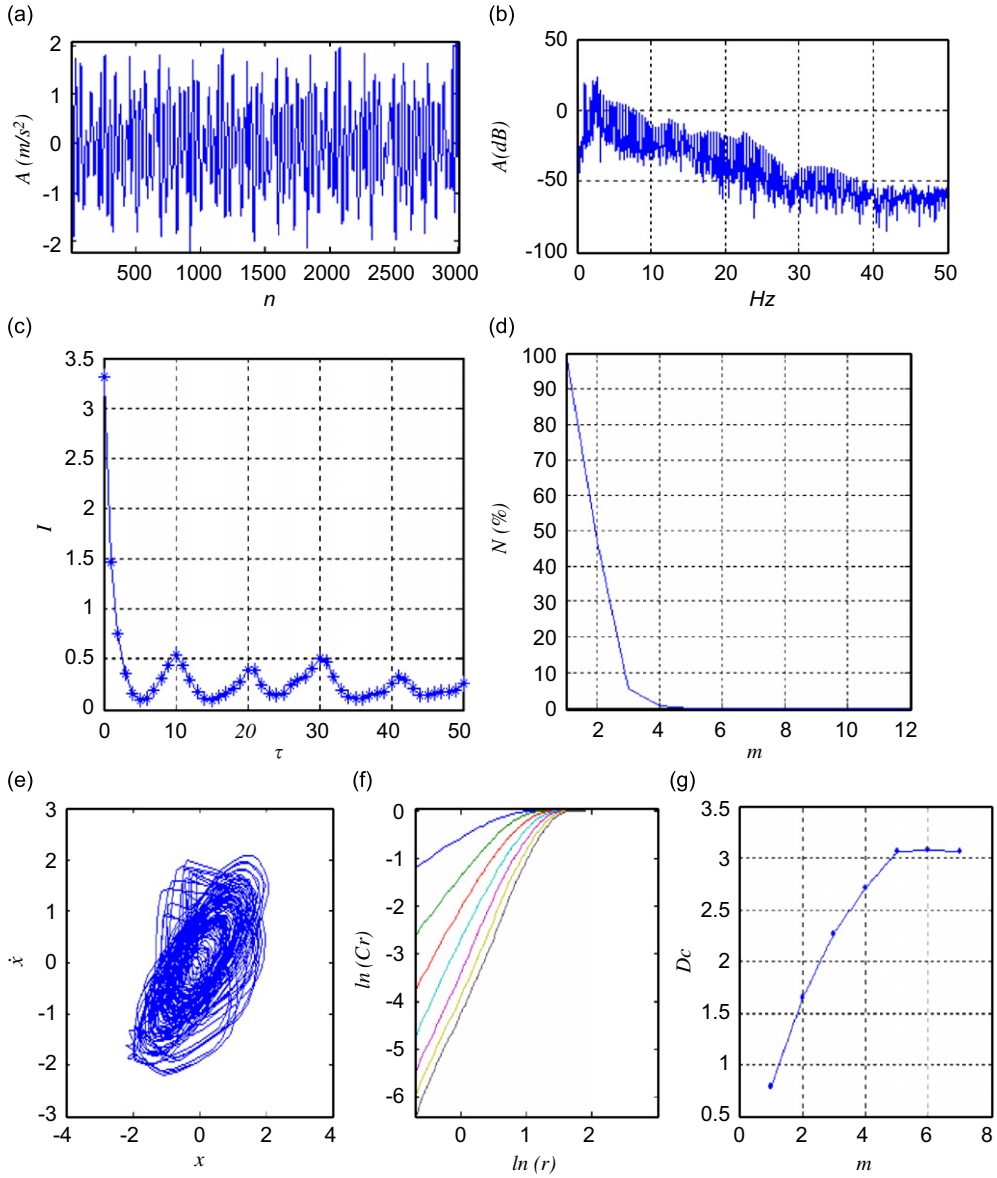

Fig. 7. Experiment results of the NVIS (a) time history, (b) power spectrum, (c) average mutual information curve, (d) FNN curve, (e) reconstructed attractor of NVIS, (f) correlation curve with G-P algorithm and (g) slopes of the curves in (f).

The trajectories of the attractor are also affected by τ. When it is small, the phase trajectories are compressed in a diagonal direction and the attractor contains only little information [19]. If τ is increased, the compressed attractor expands gradually. However, when time lag τ is lager than a certain value, the attractor is distorted in the space. Therefore, a suitable τ can ensure that the attractor unfolds fully and contains abundant useful information. To choose an optimal time lag, the first minimum of average mutual information is applied in the paper. For embedding dimension, the main task is to provide a Euclidean space R^d large enough so that the attractor can be unfolded without ambiguity. If d is too small, the attractor is folded and much information is lost. If d is too large, the calculation and the effect of noise increase greatly. Therefore, a suitable embedding dimension is expected to make sure that the attractor expands fully and the effect of the noise can be reduced greatly. Many methods including singular value decomposition can be applied to decide embedding dimension. Here the method of false neighbors is used. In the experiment, the excitation frequency is 4.5 Hz. When the gain coefficient is 0.85, the acceleration signal is measured by the LMS system, and the sample frequency is 100 Hz. The time history is shown in Fig. 7a, it is irregular just like random signal. The frequency spectra are broad band one, as shown in Fig. 7b. The first minimum of average mutual information is use to calculate the delay time and the embedding dimension is determined by the FNN. The delay time is 5, and the embedding dimension is 5, as shown in Figs. 7c and d. The reconstructed attractor phase plane diagram is shown in Fig. 7e, and the correlation dimension is 3.08, which is shown in Figs. 7f and g. It is obvious that the correlation dimension [20] of the measured time series is saturated as the embedding dimension is increased, which is different from random signal.

7. Conclusions

Based on the NVIS, the linear feedback scheme is discussed in detail. Results show that when the excitation frequency is varied, the system response can change from periodic to chaotic. When the system works in a special frequency, the variation of the gain coefficient can result in the chaos anti-control. The bifurcation diagram of the system is presented, and the strange attractor is obtained at some parameter values. In order to check the correction of the chaos anti-control method, an experiment about linear feedback is carried out on the self-design experimental rig, and the measured signal is analyzed with the nonlinear time series analysis method. At first, the first minimum of average mutual information is applied to determine the delay time and the FNN method is used to determine the embedding dimension. As a result, the delay time is 5, and the embedding dimension is 5. The characteristic exponent is calculated by the phase space reconstruction. As shown in Fig. 7f, the correlation curve converges as the embedding dimension increases. It is different from the random noise. And the correlation dimension is obtained 3.08 according to the G-P algorithm. The Lyapunov exponent is calculated as well and the value is 0.1297 which is positive. According to the analysis above, the system response is chaotic.

References

[1] E. Ott, C. Grebogi, J.A. York, Controlling chaos, *Physical Review Letter* 64 (11) (1990) 1196–1199.
[2] T. Yang, L.O. Chua, Impulsive control and synchronization of nonlinear dynamical systems and applications to secure communications, *International Journal of Bifurcation and Chaos* 7 (3) (1997) 645–664.
[3] X.F. Wang, G.R. Chen, On feedback anticontrol of discrete chaos, *International Journal of Bifurcation and Chaos* 9 (7) (1999) 1435–1441.
[4] X.F. Wang, G.R. Chen, Chaotification via arbitrarily small feedback controls: theory, method, and applications, *International Journal of Bifurcation and Chaos* 10 (3) (2000) 549–570.
[5] G.Q. Zhong, K.F. Man, G.R. Chen, Generating chaos via a dynamical controller, *International Journal of Bifurcation and Chaos* 11 (3) (2001) 865–869.
[6] K.S. Tang, K.F. Man, G.Q. Zhong, G.R. Chen, Generating chaos via $x|x|$, *IEEE Transactions on Circuits and Systems* 48 (5) (2001) 636–641.
[7] X.F. Wang, G.R. Chen, K.F. Man, Making a continuous-time minimum phase system chaotic by time-delay feedback, *IEEE Transactions on Circuit and Systems* 48 (5) (2001) 641–645.
[8] X.F. Wang, G.R. Chen, Chaotifying a stable LTI system by tiny feedback control, *IEEE Transactions on Circuit and Systems* 47 (3) (2000) 410–414.
[9] L. Yang, Z. Liu, G. Chen, Chaotifying a continuous-time system via impulsive input, *International Journal of Bifurcation and Chaos* 12 (5) (2002) 1121–1128.

[10] J.-G. Lou, S.-J. Zhu, L. He, X. Yu, Application of chaos method to line spectra reduction, *Journal of Sound and Vibration* 286 (2005) 645–652.
[11] Shu-Yong Liu, Shi-Jian Zhu, Xiangyu, Jing-Jun Lou, Study on chaotic parameter range of nonlinear vibration isolation system[C]. Progress in Safety Science and Technology, Vol. 4: Proceedings of the 2004 International Symposium on Safety Science and Technology, Tianjian, China, October 25–28, 2004.
[12] Y. Ueda, Steady motions exhibited by Duffing's equation—a picture book of regular and chaotic motions [C]. *The Engineering Foundation Conference on New Approaches to Nonlinear Problems in Dynamics,* Monterey, CA, 1979.
[13] Y. Ueda, Randomly Transitional phenomena in the systems governed by Duffing's equation, *Journal of Statistical Physics* 20 (1979) 181–196.
[14] Y. Ueda, Explorations of strange attractors exhibited by Duffing's equation, *Annals of the New York Academy of Sciences* 357 (1980) 422–434.
[15] P.J. Holmes, A Nonlinear Oscillator with a Strange Attractor. Philosophical Transactions of the Royal Society of London, *Mathematical Physics and Engineering Science A* 1394 (292) (1979) 419–448.
[16] E.H. Dowell, C. Pezeshki, On the understanding of chaos in Duffing's equation including a comparison with experiment, *Journal of Applied Mechanics* 53 (1) (1986) 5–9.
[17] A. Wolf, J.B. Swift, H.L. Swinney, J.A. Vastano, Determining Lyapunov exponent from a time series, *Physica D* 16 (1985) 285–317.
[18] A.M. Fraser, H.L. Swinney, Independent coordinates for strange attractors from mutual information, *Physical Review A* 33 (1986) 1134–1140.
[19] H.D.I. Abarbanael, The analysis of observed chaotic data in physical systems, *Reviews of Modern Physics* 65 (1993) 1348–1351.
[20] P. Grassberger, I. Procaccia, Characterization of strange of attractors, *Physical Review Letters* 50 (1983) 346–349.